Static and Dynamical Properties of the Spin-1/2 Equilateral Triangular-Lattice Antiferromagnet $Ba_3CoSb_2O_9$

J. Ma,[1,2] Y. Kamiya,[3] Tao Hong,[2] H. B. Cao,[2] G. Ehlers,[2] W. Tian,[2]
C. D. Batista,[4] Z. L. Dun,[1] H. D. Zhou,[1,5] and M. Matsuda[2]

[1]*Department of Physics and Astronomy, University of Tennessee, Knoxville, Tennessee 37996, USA*
[2]*Quantum Condensed Matter Division, Oak Ridge National Laboratory, Oak Ridge, Tennessee 37831, USA*
[3]*iTHES Research Group and Condensed Matter Theory Laboratory, RIKEN, Wako, Saitama 351-0198, Japan*
[4]*Theoretical Division, T-4 and CNLS, Los Alamos National Laboratory, Los Alamos, New Mexico 87545, USA*
[5]*National High Magnetic Field Laboratory, Florida State University, Tallahassee, Florida 32310-3706, USA*

(Received 18 July 2015; revised manuscript received 30 November 2015; published 24 February 2016)

We present single-crystal neutron scattering measurements of the spin-1/2 equilateral triangular-lattice antiferromagnet $Ba_3CoSb_2O_9$. Besides confirming that the Co^{2+} magnetic moments lie in the ab plane for zero magnetic field and then determining all the exchange parameters of the minimal quasi-2D spin Hamiltonian, we provide conclusive experimental evidence of magnon decay through observation of intrinsic line broadening. Through detailed comparisons with the linear and nonlinear spin-wave theories, we also point out that the large-S approximation, which is conventionally employed to predict magnon decay in noncollinear magnets, is inadequate to explain our experimental observation. Thus, our results call for a new theoretical framework for describing excitation spectra in low-dimensional frustrated magnets under strong quantum effects.

DOI: 10.1103/PhysRevLett.116.087201

Introduction.—The $S=1/2$ triangular-lattice Heisenberg antiferromagnet (TLHAF) is the paradigmatic example of a two-dimensional (2D) frustrated quantum magnet [1–14]. The combination of frustration, strong quantum fluctuations, and low dimensionality is anticipated to produce strong deviations from semiclassical theories. While several distorted triangular-lattice materials, such as κ-$(BEDT\text{-}TTF)_2Cu_2(CN)_3$ [15], Cs_2CuX_4 ($X=Cl$ [16–18] and Br [18–20]), and $CuCrO_2$ [21,22], have been investigated in the past, the distorted structures introduce additional terms, such as the Dzyaloshinskii-Moriya (DM) interaction, into the paradigmatic Hamiltonian [16–20,23].

The equilateral triangular-lattice quantum antiferromagnet $Ba_3CoSb_2O_9$ was synthesized recently [24–29]. The Co^{2+} ion has a Kramers doublet ground state due to the spin-orbit coupling, and this doublet can be described as an effective spin-1/2 moment. In addition, the high symmetry of the hexagonal crystal structure, $P6_3/mmc$ [24–28], forbids DM interaction for pairs up to third nearest-neighbor (NN) in the same ab-plane and between any pair of spins along the c axis [25].

Powder neutron diffraction measurements presented the noncollinear 120° structure with the magnetic wave vector $\mathbf{Q}=(1/3,1/3,1)$ [24]. The Néel temperature was found to be ≈3.8 K and a rich temperature-magnetic field phase diagram was reported up to 32 T [25–28]. Electronic spin resonance (ESR) [27] and nuclear magnetic resonance (NMR) [28] measurements suggested a spin model with small easy-plane exchange anisotropy and an exchange interaction along the c axis much weaker than the NN intralayer exchange. This observation is consistent with the alternation of magnetic (Co^{2+}) and nonmagnetic (Sb_2O_9 polyhedra) layers along the c direction. While more precise determination of the model parameters requires inelastic neutron scattering (INS) measurements, such detailed information is, indeed, physically relevant. The reason is that, according to the semiclassical theories in Refs. [8,9], "smoking gun" features of the magnetic excitations of the 2D $S=1/2$ TLHAF, such as the line broadening of the single-magnon excitations resulting from spontaneous magnon decays [7–10,30], can be rather sensitive to small deviations from the ideal model.

In this Letter, we present direct evidence of the magnetic structure in $Ba_3CoSb_2O_9$ and the detailed profile of magnon excitations obtained by neutron scattering measurements. We confirm the 120° order lying in the ab plane at zero field [27,28] and determine the exchange constants of the minimal quasi-2D XXZ Hamiltonian proposed in Refs. [12,27,28]. The INS spectrum also exhibits intrinsic line broadening. By comparing the INS profile against the linear spin-wave (LSW) theory and the LSW + $1/S$ corrections, we show that quantum fluctuations produce the theoretically predicted renormalizations of the magnon dispersion [6,7]. More importantly, however, our thorough examination reveals that the semiclassical (i.e., large S) treatment is inadequate to explain the observed magnon decay and the associated line broadening in this spin-1/2 system, thereby pointing to a need for developing an alternative theoretical framework. Thus, although quantum fluctuations are not enough to destroy magnetic ordering in

$Ba_3CoSb_2O_9$, this Letter indicates that these fluctuations are qualitatively modifying the excitation spectrum relative to the semiclassical (large-S) regime.

Experiments.—The single crystal of $Ba_3CoSb_2O_9$ [~1 g, diameter (5 mm) × length (15 mm)] was grown by the floating-zone technique and oriented in the (*hhl*) scattering plane for INS measurements. The unpolarized neutron diffraction data were obtained using the HB-1A triple-axis spectrometer (TAS) and the HB-3A four circle diffractometer at High Flux Isotope Reactor (HFIR), Oak Ridge National Laboratory (ORNL) [31]. The absence of site disorder between Co and Sb was confirmed within an error of 1% and the magnetic wave vector (**Q**) is [1/3, 1/3, 1] [24]. We collected twenty magnetic Bragg peaks at 1.7 K, and refined the data with FULLPROF [32]. Two variants of the 120° structure were compared as the "*ab*" and "*ac*" plane models, which are favored by easy-plane and easy-axis anisotropy, respectively [11,12,33]. The *ab* plane model corresponds to a 120° structure with all spins in the *ab* plane [Fig. 1(a)], while the *ac* plane model assumes the 120° structure with one third of the moments parallel or antiparallel to the *c* axis [Fig. 1(b)]. Although the same magnetic Bragg peaks were generated from both structures, the related scattering intensity profiles were different. Our data are consistent with the *ab* plane model, Figs. 1(a) and 1(b).

We measured a series of magnetic Bragg peaks, [1/3 1/3 1], [2/3 2/3 1], [1/3 1/3 3], and [1/3 1/3 5], and nuclear peaks, [110] and [006], using the HB-1 polarized neutron TAS at HFIR, ORNL for further confirmation of the spin directions. Figures 1(c) and 1(d) show the [1/3 1/3 3] and [2/3 2/3 1] peaks, respectively. Since they are observed in the spin-flip channel with the initial polarization vector **P** parallel to the scattering vector **q**, both peaks are magnetic. More information on the magnetic order can be obtained by the neutrons polarized along the $[1\bar{1}0]$ direction, which is perpendicular to the (*hhl*) plane, and then evaluating the intensity ratio I_{SF}/I_{NSF} between the spin-flip (SF) and non-spin-flip (NSF) channels. In our configuration, the SF (NSF) scattering originates from the in-plane (out-of-plane) spin components. This analysis (Table I) confirms the *ab* plane model, in agreement with the easy-plane anisotropy proposed in the ESR [27] and NMR [28] measurements in disagreement with Refs. [24–26,34].

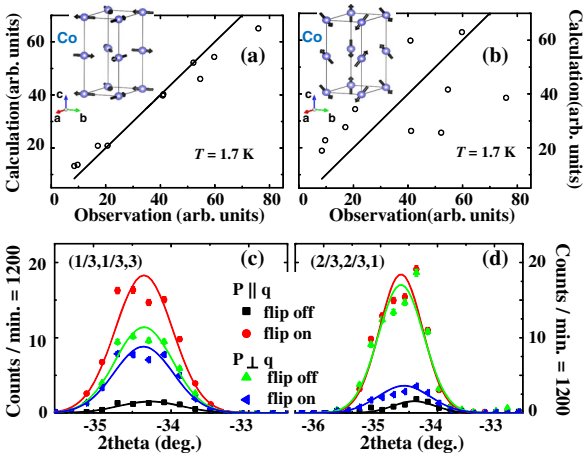

FIG. 1. Comparison between the observed magnetic Bragg peak intensities at 1.7 K on the HB-1A TAS and the simulated ones based on the 120° structure in the (a) *ab* plane and (b) *ac* plane. The solid lines are guides to the eye. Magnetic Bragg peaks at (c) [1/3 1/3 3] and (d) [2/3 2/3 1] measured with polarized neutrons at 1.7 K on HB-1. The backgrounds have been subtracted. **P** and **q** are the polarization and the scattering vector, respectively.

To investigate the spin dynamics in $Ba_3CoSb_2O_9$, we performed INS measurements on CG-4C cold neutron TAS at HFIR and Cold Neutron Chopper Spectrometer (CNCS) at Spallation Neutron Source, ORNL. At the CG-4C TAS, the final energy was fixed at either 5 or 3.5 meV. The incident energy on CNCS was fixed at 3.315 meV. Figures 2(a)–2(c) show the scattering profile at 1.5 K along high-symmetry directions in the reciprocal space. Three dominant modes are observed as expected for the 120° structure. To be consistent with the theoretical calculation, Miller indices in the following texts are labeled by the model notation.

The overall bandwidth of discernible single-magnon branches is around 1.7 meV for the in-plane dispersion. Our measurements also resolved the finite bandwidth ≈1.1 meV along the *c* axis for the Goldstone mode [Fig. 2(c)], which implies a non-negligible interlayer antiferromagnetic exchange. The relevance of the finite interlayer exchange was pointed out recently [12,28] to explain a weak anomaly in the magnetization curve at around 22 T for a magnetic field **B** parallel to the *ab* plane [27]. The corresponding anomaly was clearly observed by NMR [28]. The gap of the quadratic band at $\mathbf{q} = [2/3, -2/3, -1]$ is around 0.65 meV, which agrees well with 170 GHz by ESR [27]. Around $\mathbf{q} = [1/2, 0, -1]$ (M_1 point), we observed rotonlike minima and a flat mode, such as in the dispersion along $K_1' \rightarrow M_1 \rightarrow Y_1$ or $X_1 \rightarrow M_1 \rightarrow \Gamma_1$ [Fig. 2(a)].

The most interesting feature of the magnetic excitations is the line broadening observed throughout the whole Brillouin zone (BZ) (Fig. 2), which was missed due to the instrument and sample limitations in Ref. [26]. As

TABLE I. Ratios between the spin-flip and non-spin-flip scattering intensities measured with neutrons polarized perpendicular to the scattering wave vector **q**.

		Magnetic model calculations	
Index	I_{SF}/I_{NSF}	*ab* plane model	*ac* plane model
[2/3 2/3 1]	0.16(2)	0.12	0.88
[1/3 1/3 1]	0.36(3)	0.33	0.67
[1/3 1/3 3]	0.81(2)	0.82	0.18
[1/3 1/3 5]	0.94(2)	0.92	0.08

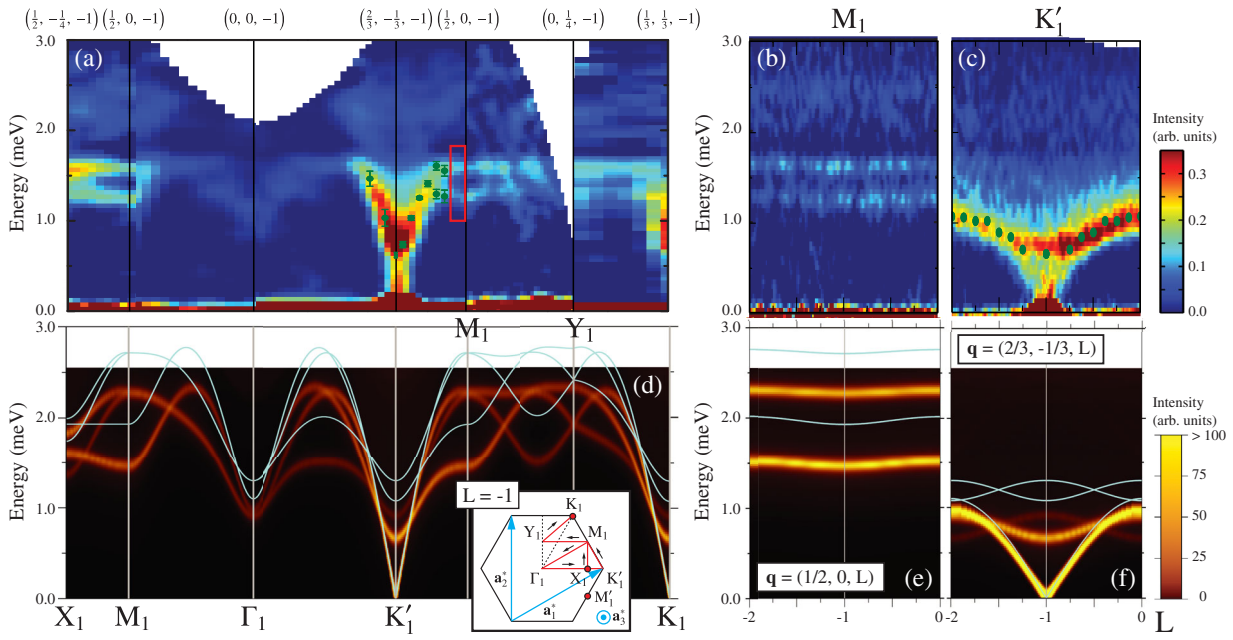

FIG. 2. INS spectra of $Ba_3CoSb_2O_9$ as a function of the momentum and energy transfer at $T = 1.5$ K along the high symmetric (a) intralayer directions and the interlayer (b) $[1/2, 0, \mathrm{L}]$, and (c) $[2/3, -1/3, \mathrm{L}]$ directions in the reciprocal space. The background has been subtracted. The filled circles are peak positions from the measurements at the CG-4C TAS. The red rectangular frame in (a) represents the region where the decay effect is distinct and the details are discussed in Fig. 3(a). (d)–(f) The intensity plot of the dynamical structure factor along the same symmetry lines as in (a)–(c) for $J = 1.7$ meV, $J'/J = 0.05$, and $\Delta = 0.89$ at $T = 0$ calculated with the non-linear spin-wave approximation. The energy resolution (0.063 meV) has been convoluted. The solid lines represent the poles in the LSW approximation.

demonstrated in the constant-$\mathbf{q}$ plots near the M_1 point, $\mathbf{q} = [1/2, 0, -1]$, the linewidths are several times broader than the instrument resolution [Fig. 3(a)]. As discussed in Ref. [31], we have excluded the possible extrinsic broadening factors, such as the sample inhomogeneities, the instrument resolution and data rebinning effects. Similar line broadening was reported in the 2D trimerized triangular antiferromagnet $LuMnO_3$ [35]. In Fig. 3(b), we show the constant-frequency cut at $\hbar\omega = 1.3$ meV focused on the BZ boundary. Besides the triangular-shaped intensity around the K_1 and K_1' points corresponding to a nearly flat single-magnon excitation [10], we observed a relatively blurred circular-shaped intensity. This feature resembles the one observed in the prototypical 2D TLHAF model [10]. In addition to these broadened quasiparticle peaks, we observed more diffusive features at higher frequency $\hbar\omega \gtrsim 2$ meV [Figs. 2(a)–2(c)], which are likely due to the longitudinal spin fluctuations associated with a two-magnon continuum. Finally, we found that the Goldstone mode emanating from the Bragg spot $\mathbf{q} = [2/3, -1/3, -1]$ has a rather weak intensity compared to the quadratic gapped branch. Although we believe this is not an experimental artifact, this observation is rather unusual.

Spin-wave theory.—The INS results were analyzed by the LSW theory and the LSW + $1/S$ corrections based on the spin-1/2 quasi-2D XXZ Hamiltonian on a vertically stacked triangular lattice

$$\mathcal{H} = J\sum_{\langle \mathbf{r},\mathbf{r}'\rangle}(S^x_{\mathbf{r}}S^x_{\mathbf{r}'} + S^y_{\mathbf{r}}S^y_{\mathbf{r}'} + \Delta S^z_{\mathbf{r}}S^z_{\mathbf{r}'}) + J'\sum_{\mathbf{r}}(S^x_{\mathbf{r}}S^x_{\mathbf{r}+\hat{z}} + S^y_{\mathbf{r}}S^y_{\mathbf{r}+\hat{z}} + \Delta S^z_{\mathbf{r}}S^z_{\mathbf{r}+\hat{z}}). \quad (1)$$

Here, $\langle \mathbf{r}, \mathbf{r}'\rangle$ runs over the in-plane NNs. J and J' ($J, J' > 0$) are the intra- and interlayer NN antiferromagnetic exchange, respectively. $\Delta < 1$ parametrizes the easy-plane

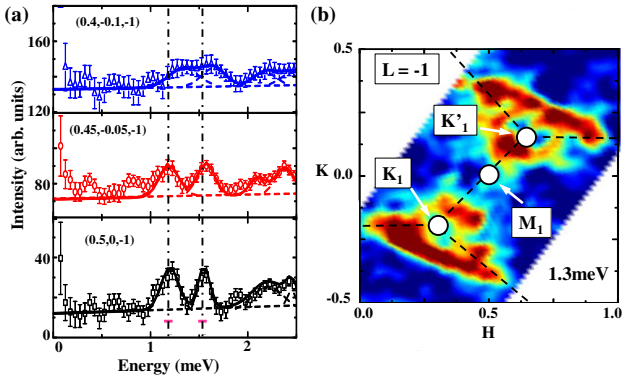

FIG. 3. (a) The constant- $\mathbf{q}$ scans near M_1 point, $\mathbf{q} = [1/2, 0, -1]$. The horizontal error bars indicate the instrumental resolution. Thin dashed lines indicate individual fitted Gaussian peaks and background, and the solid line is their sum. The very broad feature above 2 meV may be attributed to the two-magnon continuum. (b) The constant-energy cut at 1.3 meV as a function of $\mathbf{q}$=$(H, K, L = -1)$. The dashed lines are the BZ boundaries.

exchange anisotropy. This is a minimal extension of the isotropic 2D TLHAF model ($J' = 0$ and $\Delta = 1$) [6–10]. The classical ground state for $J' > 0$ and $\Delta < 1$ coincides with the experimentally observed 120° structure. A tentative rough estimate $J \approx 1.6$ meV can be made by comparing the saturation field value (32.8 T for $\mathbf{B}\|\hat{\mathbf{c}}$ [27]) with $g\mu_B B_{\rm sat} = [3(1+2\Delta)J + 2(1+\Delta)J']S$ assuming J'/J, $1-\Delta \ll 1$ and $g = 3.87$ for $\mathbf{B}\|\hat{\mathbf{c}}$ [27]. This suggests the temperature for our INS measurements to be $T \approx 0.1J$.

The spin-wave theory is derived by the standard Holstein-Primakoff transformation relative to the 120° structure. The LSW dispersion, $\omega_0(\mathbf{q})$, is obtained by diagonalizing the quadratic part of the spin-wave Hamiltonian. The spiral 120° ordering leads to three branches of poles in the dynamical spin structure factor at $\omega_0(\mathbf{q})$ and $\omega_0(\mathbf{q} \pm \mathbf{Q})$ [the solid lines in Figs. 2(d)–2(f)]. Several qualitative features of the spectrum can already be captured at this LSW level. First, the gap (≈0.65 meV) of the quadratic branch at $\mathbf{q} = [2/3, -1/3, -1]$ is induced by the easy-plane exchange anisotropy. This gap is proportional to $\sqrt{1-\Delta}$. The bandwidth of the Goldstone mode along the [001] direction is $\propto \sqrt{J'/J}$, implying that a rather small value of J'/J can explain the observed bandwidth (≈1.1 meV) [Fig. 2(c)]. These observations remain robust after including the next order corrections in $1/S$ [31]. The overlap near $\mathbf{q} = [2/3, -1/3, 0]$ of the gapped and gapless high intensity branches along $\mathbf{q} = [2/3, -1/3, \mathrm{L}]$ is another characteristic of $Ba_3CoSb_2O_9$ [Fig. 2(c)].

To quantify the effect of quantum fluctuations on the single-magnon spectrum, we include the next order in $1/S$ to compute the dynamical structure factor $\mathcal{S}(\mathbf{q},\omega) = (2\pi N)^{-1}\sum_{\mathbf{r},\mathbf{r}'}\int_{-\infty}^{\infty} dt e^{i[\omega t - \mathbf{q}\cdot(\mathbf{r}-\mathbf{r}')]}\langle \mathbf{S}_{\mathbf{r}}(t)\cdot\mathbf{S}_{\mathbf{r}'}(0)\rangle$ (N is the total number of Co^{2+} ions) at $T = 0$. The result is shown in Figs. 2(d)–2(f), where the experimental energy resolution (≈0.063 meV) has been convoluted [31]. This quantum correction arises from the cubic terms that appear in the spin-wave Hamiltonian because of the noncollinear nature of the spin ordering and from a Hartree-Fock decoupling of the always present quartic terms [7–10,30]. The parameters of our best fitting are $J = 1.7$ meV, $J'/J = 0.05$, and $\Delta = 0.89$. They are chosen to reproduce the gap of the quadratic branch at $\mathbf{q} = [2/3, -1/3, -1]$, the bandwidth of the Goldstone mode along the [001] direction, and the saturation field for $\mathbf{B}\|\hat{\mathbf{c}}$ [31]. The main difference relative to the previous estimates from ESR measurements ($J'/J = 0.026$ and $\Delta = 0.94$) [27] is the stronger exchange anisotropy. By comparing against the LSW results, we confirm the strong downward renormalization [as large as ≈40% near $\mathbf{q} = [2/3, -1/3, -1]$] of the single-magnon dispersion. This is a salient feature of frustrated low-spin magnets relative to unfrustrated systems. For instance, the renormalization due to $1/S$ corrections is upward in the square-lattice $S = 1/2$ antiferromagnetic Heisenberg model [36]. A rather small downward renormalization of ≈5% is observed in the $S = 2$ triangular lattice compound $LuMnO_3$ because of the rather large value of the spin [35].

While many key features of the measured spectra are well captured by our minimal model, there are several noteworthy discrepancies. First, as expected, the calculation yields high intensity for the Goldstone mode. Second, while the shape of the low-frequency dispersion ($\lesssim$1.5 meV) is well reproduced, the calculation overestimates the energy of the high-frequency part (e.g., ≈2.3 meV near the M_1 point, whereas it is ≈1.7 meV experimentally). This overestimate is a robust feature of our minimal Hamiltonian (1) at both LSW and LSW + $1/S$ levels [31]. We examined the effect of the antiferromagnetic next-nearest-neighbor intralayer exchange J_2, which, however, lowers both energy scales, and relatively speaking, the separation between the two branches increases with J_2 [31].

More importantly, the LSW + $1/S$ calculation yields quite stable quasiparticle peaks [Figs. 2(d)–2(f)] instead of the observed line broadening in the parameter regime relevant for $Ba_3CoSb_2O_9$ [Figs. 2(a)–2(c)]. The large S theory applied to the 2D isotropic TLHAF model predicts that single magnon excitations can decay into a two-magnon continuum in a large region of the BZ where the kinematic conditions are satisfied [7–10,30]. Such magnon decays make the magnon lifetime finite and cause the line broadening. However, the non-negligible easy-plane exchange-anisotropy in $Ba_3CoSb_2O_9$ implies that this semiclassical scenario fails to reproduce the experimental observation because, as already pointed out in Refs. [8,9], the associated gap opening violates the kinematic condition in the increasingly large area of the BZ [31]. In addition, the interlayer coupling also acts against spontaneous magnon decays. One possibility is that we are missing some significant interactions in our minimal Hamiltonian (1). An alternative explanation is that semiclassical approaches are simply inadequate to describe magnon decay in low-dimensional frustrated spin systems with small S.

Conclusions.—In summary, our neutron diffraction measurements of single-crystal $Ba_3CoSb_2O_9$ confirm that the zero-field magnetic ordering is a 120° structure in the ab plane. By comparing our measurements against the dynamical spin structure factor obtained from the LSW + $1/S$ treatment of a stacked triangular-lattice $S = 1/2$ XXZ model, we extracted both exchange and anisotropy parameters. Our results indicate that $Ba_3CoSb_2O_9$ is an almost ideal realization of an equilateral $S = 1/2$ TLHAF. The measured INS profile exhibits several salient features theoretically predicted for frustrated quantum magnets, such as the strong downward renormalization of the magnon dispersion, rotonlike minima, flat modes near the BZ boundary, and the line broadening throughout the entire BZ. However, our detailed comparison between the experiments and the large S treatments reveals that the observed magnon decay in $Ba_3CoSb_2O_9$

cannot be explained with a semiclassical treatment. Thus, this Letter shows that a new theoretical framework is need to describe the low-energy excitation spectrum of magnetically ordered low-dimensional frustrated magnets.

The authors acknowledge valuable discussions with M. Mourigal. The research at HFIR and SNS at ORNL were sponsored by the Scientific User Facilities Division (J. M., T. H., H. B. C., W. T., and M. M.), Office of Basic Energy Sciences, U.S. Department of Energy. J. M., Z. L. D., and H. D. Z. acknowledge support from NSF-DMR through Grant No. DMR-1350002 and from NHMFL through Grant No. NSF-DMR-1157490, U.S. DOE, and the State of Florida. Y. K. acknowledges financial supports from the RIKEN iTHES project. Work at LANL was performed under the auspices of the U.S. DOE Contract No. DE-AC52-06NA25396 through the LDRD program.

[1] L. Balents, Nature (London) **464**, 199 (2010).
[2] R. Moessner and A. P. Ramirez, Phys. Today **59**, 24 (2006).
[3] P. W. Anderson, Mater. Res. Bull. **8**, 153 (1973).
[4] P. Fazekas and P. W. Anderson, Philos. Mag. **30**, 423 (1974).
[5] A. Mezio, L. O. Manuel, R. R. P. Singh, and A. E. Trumper, New J. Phys. **14**, 123033 (2012).
[6] W. Zheng, J. O. Fjærestad, R. R. P. Singh, R. H. McKenzie, and R. Coldea, Phys. Rev. B **74**, 224420 (2006).
[7] O. A. Starykh, A. V. Chubukov, and A. G. Abanov, Phys. Rev. B **74**, 180403(R) (2006).
[8] A. L. Chernyshev and M. E. Zhitomirsky, Phys. Rev. Lett. **97**, 207202 (2006).
[9] A. L. Chernyshev and M. E. Zhitomirsky, Phys. Rev. B **79**, 144416 (2009).
[10] M. Mourigal, W. T. Fuhrman, A. L. Chernyshev, and M. E. Zhitomirsky, Phys. Rev. B **88**, 094407 (2013).
[11] D. Yamamoto, G. Marmorini, and I. Danshita, Phys. Rev. Lett. **112**, 127203 (2014).
[12] D. Yamamoto, G. Marmorini, and I. Danshita, Phys. Rev. Lett. **114**, 027201 (2015).
[13] D. Sellmann, X. F. Zhang, and S. Eggert, Phys. Rev. B **91**, 081104(R) (2015).
[14] E. A. Ghioldi, A. Mezio, L. O. Manuel, R. R. P. Singh, J. Oitmaa, and A. E. Trumper, Phys. Rev. B **91**, 134423 (2015).
[15] Y. Shimizu, K. Miyagawa, K. Kanoda, M. Maesato, and G. Saito, Phys. Rev. Lett. **91**, 107001 (2003).
[16] R. Coldea, D. A. Tennant, and Z. Tylczynski, Phys. Rev. B **68**, 134424 (2003).
[17] O. Breunig, M. Garst, A. Rosch, E. Sela, B. Buldmann, P. Becker, L. Bohatý, R. Müller, and T. Lorenz, Phys. Rev. B **91**, 024423 (2015).
[18] N. van Well, K. Foyevtsova, S. Gottlieb-Schönmeyer, F. Ritter, R. S. Manna, B. Wolf, M. Meven, C. Pfleiderer, M. Lang, W. Assmus, R. Valentí, and C. Krellner, Phys. Rev. B **91**, 035124 (2015).
[19] T. Ono, H. Tanaka, H. Aruga Katori, F. Ishikawa, H. Mitamura, and T. Goto, Phys. Rev. B **67**, 104431 (2003).
[20] N. A. Fortune, S. T. Hannahs, Y. Yoshida, T. E. Sherline, T. Ono, H. Tanaka, and Y. Takano, Phys. Rev. Lett. **102**, 257201 (2009).
[21] M. Poienar, F. Damay, C. Martin, J. Robert, and S. Petit, Phys. Rev. B **81**, 104411 (2010).
[22] M. Frontzek, J. T. Haraldsen, A. Podlesnyak, M. Matsuda, A. D. Christianson, R. S. Fishman, A. S. Sefat, Y. Qiu, J. R. D. Copley, S. Barilo, S. V. Shiryaev, and G. Ehlers, Phys. Rev. B **84**, 094448 (2011).
[23] O. A. Starykh, H. Katsura, and L. Balents, Phys. Rev. B **82**, 014421 (2010).
[24] Y. Doi, Y. Hinatsu, and K. Ohoyama, J. Phys. Condens. Matter **16**, 8923 (2004).
[25] Y. Shirata, H. Tanaka, A. Matsuo, and K. Kindo, Phys. Rev. Lett. **108**, 057205 (2012).
[26] H. D. Zhou, C. Xu, A. M. Hallas, H. J. Silverstein, C. R. Wiebe, I. Umegaki, J. Q. Yan, T. P. Murphy, J.-H. Park, Y. Qiu, J. R. D. Copley, J. S. Gardner, and Y. Takano, Phys. Rev. Lett. **109**, 267206 (2012).
[27] T. Susuki, N. Kurita, T. Tanaka, H. Nojiri, A. Matsuo, K. Kindo, and H. Tanaka, Phys. Rev. Lett. **110**, 267201 (2013).
[28] G. Koutroulakis, T. Zhou, Y. Kamiya, J. D. Thompson, H. D. Zhou, C. D. Batista, and S. E. Brown, Phys. Rev. B **91**, 024410 (2015).
[29] G. Quirion, M. Lapointe-Major, M. Poirier, J. A. Quilliam, Z. L. Dun, and H. D. Zhou, Phys. Rev. B **92**, 014414 (2015).
[30] M. E. Zhitomirsky and A. L. Chernyshev, Rev. Mod. Phys. **85**, 219 (2013).
[31] See Supplemental Material at http://link.aps.org/supplemental/10.1103/PhysRevLett.116.087201 for details.
[32] J. Rodriguez-Carvajal, Physica (Amsterdam) **192B**, 55 (1993).
[33] S. Miyashita, J. Phys. Soc. Jpn. **55**, 3605 (1986).
[34] The phase diagram in Ref. [26] is consistent with the recent studies [27,28] after adopting $\hat{a} \leftrightarrow \hat{c}$.
[35] J. Oh, M. D. Le, J. Jeong, J. H. Lee, H. Woo, W. Y. Song, T. G. Perring, W. J. L. Buyers, S.-W. Cheong, and J. G. Park, Phys. Rev. Lett. **111**, 257202 (2013).
[36] J.-i. Igarashi and T. Nagao, Phys. Rev. B **72**, 014403 (2005).